7-3-2017

Unraveling the Coulombic Forces in Electronically Decoupled Bichromophoric Systems during Two Successive Electron Transfers

Maxim V. Ivanov
Marquette University

Shriya Wadumethrige
Marquette University

Denan Wang
Marquette University, denan.wang@marquette.edu

Rajendra Rathore
Marquette University, rajendra.rathore@marquette.edu

Unraveling the Coulombic Forces in Electronically Decoupled Bichromophoric Systems during Two Successive Electron Transfers

Maxim V. Ivanov
Department of Chemistry, Marquette University, Milwaukee, WI
Shriya H. Wadumethrige
University of Ruhuna, Sri Lanka
Denan Wang
Department of Chemistry, Marquette University, Milwaukee, WI
Rajendra Rathore
Department of Chemistry, Marquette University, Milwaukee, WI

Abstract

Coulombic forces are vital in modulating the electron transfer dynamics in both synthetic and biological polychromophoric assemblies, yet quantitative studies of the impact of such forces are rare, as it is difficult to disentangle electrostatic forces from simple electronic coupling. To address this problem, the impact of Coulombic interactions in the successive removal of two electrons from a model set of spirobifluorenes, where the interchromophoric electronic coupling is nonexistent, is quantitatively assessed. By systematically varying the separation of the bifluorene moieties using model compounds, ion pairing, and solvation, these interactions, with energies up to about 0.4 V, are absent at distances greater than about 9 Å. These findings can be (quantitatively) applied for the design of polychromophoric assemblies, whereby the redox properties of donors and/or acceptors can be tuned by judicious positioning of the charged groups to control the electron-transfer dynamics.

Polychromophoric assemblies play an important role in the elucidation of electron transfer dynamics, probing the necessary structural/electronic parameters for long-range electron transfers.[1, 2] Electrochemical oxidation of such assemblies often shows multiple oxidation waves; however, it is not clear whether splitting of the oxidation waves occurs by interchromophoric electronic coupling, or Coulombic (electrostatic) interactions among the charged chromophores. For example, a hexaarylbenzene derivative (structure **A**, Figure **1**) shows six well-separated oxidation waves;[3] however, quantitatively extracting the contributions from the electronic coupling and Coulombic interactions responsible for the splitting of the oxidation waves in **A** has not been possible.
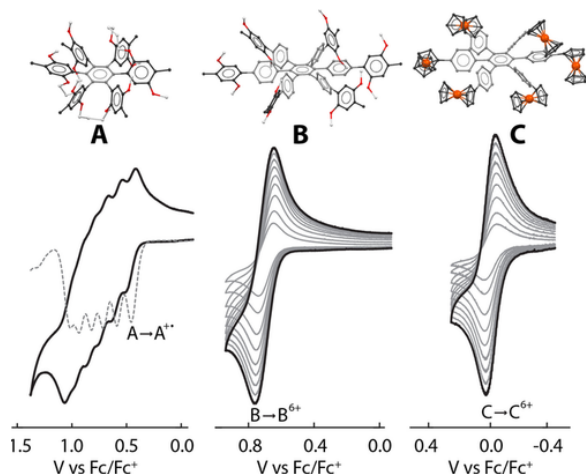

Figure 1 Cyclic voltamgramms (CVs) of hexaphenylbenzene-based polychromophoric molecules in CH_2Cl_2 (0.2 m nBu$_4$N$^+$PF$_6^-$) at v=100 mV s^{-1} (A) and 25–400 mV s^{-1} (Band C) at 22 °C.[5, 6] Use of an internal standard of similar molecular size and shape avoided the issues arising from differential diffusion,[6] and confirmed the ejection of all six electrons at the same potential in B and C.

The existence of electronic coupling among the chromophores in a molecular assembly is evidenced in a lowering of the first oxidation potential as compared to an appropriate model compound (e.g. structure **B** in Figure **2**), and the accompanying spectral signature[4] signifying hole delocalization. Indeed, six circularly arrayed aryl groups in structure **A** (Figure **2**) stabilize a cationic charge by 0.25 V as compared to a model compound.[3] Ejection of each successive electron in **A** must then overcome an

energetic penalty associated with delocalization of additional charges and minimization of the Coulombic forces among the electronically coupled charge-bearing units, as reflected in the cyclic voltammograms (CVs) (Figure **2**), which displays a series of distinct oxidation waves.

Unlike **A**, structures **B** and **C** (Figure **2**), where the electro-active 2,5-dimethoxytolyl or ferrocenyl groups are moved away from the central benzene ring by a phenylene spacer, show CVs with a single wave, consistent with ejection of all six electrons at the same oxidation potentials.[5, 6] Quantitative redox titrations,[5, 6] cyclic voltammetry with internal standards of comparable sizes,[6] together with the similarity of the electronic spectra of their polycations with appropriate model compounds, confirmed a complete absence of both interchromophoric electronic coupling and Coulombic interactions in **B** and **C**.[5, 6] A cursory examination of the molecular structures of **B** and **C** shows a separation of about 8.8 Å among the electro-active groups, sufficient to completely prevent both through-space electronic coupling[7] and Coulombic interactions.[4, 5] The Coulombic interactions are known to scale inversely with the distance between a pair of charges, however, based on examples **B** and **C**, one cannot discern the critical distance at which the Coulombic forces will trigger. Moreover, in **A** one cannot easily disentangle the relative contribution of Coulombic forces between closely juxtoposed charged chromophores in the presence of the inherent interchromophoric electronic coupling.[3]

Herein, spirobifluorenes (see Scheme **1**) are identified as bichromophoric systems, in which the orthogonal arrangement of a pair of closely juxtaposed fluorene moieties severely restricts the interchromophoric electronic coupling.[8, 9] This represents an ideal system for the evaluation of the role of Coulombic interactions in dicationic species.
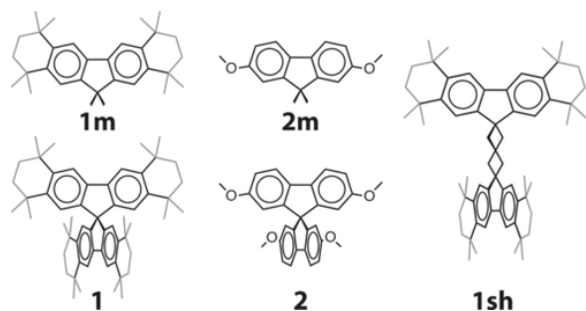

Scheme 1 Structures and numbering of various spirobifluorenes and model compounds. Lightly shaded bonds in 1 represent annulated alkyl groups.

To quantitatively evaluate the role of Coulombic interactions in spirobifluorene dications, we synthesized several derivatives that undergo reversible electrochemical oxidations and produce stable cation radicals and dications. Electrochemical analysis, electronic spectroscopy, and DFT calculations show that Coulombic forces are as large as about 0.4 V between charged fluorene moieties in spirobifluorenes, and can be modulated by increasing the distance between the chromophores, ion pairing and solvation. This fundamental quantitative study of the role of the Coulombic forces in the energetics of electron transfer in multiply charged assemblies is expected to be of critical importance for the study and design of novel polychromophoric systems for long-range charge transport, including biologically relevant assemblies.

To ensure electrochemical reversibility in the model compounds, the spirobifluorene derivatives with substitution-prone 2,7-positions blocked by alkyl (**1**) or methoxy (**2**) groups were synthesized using readily available precursors, using modified reactions typically employed for the synthesis of parent spirobifluorene (see Supporting Information for details) . A spirobifluorene derivative **1 sh**, in which the two fluorenyl rings are separated by a spiroheptane bridge, was also synthesized. The model compounds **1 m** and **2 m** were accessed from the intermediates available from the syntheses of **1** and **2**. The compounds reported herein were characterized by $^1H/^{13}C$ NMR spectroscopy, MALDI mass spectrometry, and X-ray crystallography (see Supporting Information for full details).

Electrochemical oxidation of the alkyl- (**1**) and methoxy- (**2**) substituted spirobifluorenes shows two well-separated (reversible) oxidation waves in their cyclic voltammograms (Figure **2** A, black curves), which correspond to the formation of cation radicals and dications, respectively (see Table **1**). First oxidation potentials (E_{ox1}) of **1/2** were found to be similar to those of the model compounds **1 m/2 m** (Figure **2** A, blue curves), suggesting negligible electronic coupling between the fluorene moieties in each of **1$^{+\cdot}$** and **2$^{+\cdot}$**.[10]
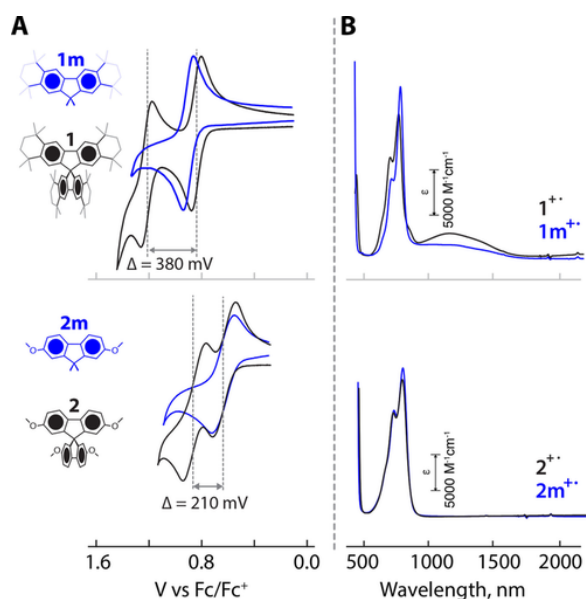
Figure 2 A) Cyclic voltammograms of 1/2 and 1 m/2 m in CH₂Cl₂ (0.1 m $nBu_4N^+PF_6^-$) at v=200 mV s^{-1} and 22 °C. B) Electronic absorption spectra of 1$^{+\cdot}$/2$^{+\cdot}$ and 1 m$^{+\cdot}$/2 m$^{+\cdot}$in CH₂Cl₂ at 22 °C. For both parts A) and B) the blue traces represent model compounds 1m/2m, and the black traces represent the spirobifluorenes 1/2.

Next, we generated the cation radicals of spirobifluorenes (**1$_+$·/2$_+$·**) and their model compounds (**1 m$^{+\cdot}$/2 m$^{+\cdot}$**) through quantitative[11, 12] redox titrations using robust aromatic oxidants (i.e. **NAP$^{+\cdot}$** and **THEO$^{+\cdot}$**)[13] in CH₂Cl₂ at ambient temperatures (see Supporting Information for details). The electronic absorption spectrum of each spirobifluorene cation radical was found to be remarkably similar to the spectrum of the respective model compound (Figure **3** B), attesting to a lack of electronic coupling between the fluorenes in **1$^{+\cdot}$**and **2$^{+\cdot}$**.[10] Thus, the splitting of the oxidation waves (namely Δ=E_{ox2}−E_{ox1}, Figure **3**) by 380 mV and 210 mV, in **1** and **2**, respectively, is brought about largely from Coulombic (electrostatic) interactions between two positively charged fluorenyl units.[14] Furthermore,

the observation that the splitting of the oxidation waves (Δ) in the methoxy-substituted **2** is almost half of the splitting in alkyl-substituted **1** was surprising, as separation of the fluorenyl units in **1** and **2** is identical (see below).

To examine the extent of electrostatic interactions and elucidate the role of varied charge distributions imposed by substitution in **1²⁺/2²⁺**, we examined the electronic structures of **1/2** and **1 m/2 m** by DFT calculations. Calculations of neutral, cation radical and dication states of **1** and **2** were performed at the B1LYP-40/6-31G(d)+PCM(CH_2Cl_2) level of theory, which we have extensively utilized for the accurate description of electronic structures of various π-conjugated cation radicals.[15] The computed [B1LYP40] difference (Δ) between oxidation energies of the removal of the first and second e⁻ for **1²⁺/2²⁺** were overestimated by about 200–300 mV when compared with experimental values (see Table [1]). A similar overestimation was found with other commonly utilized standard functionals (see Table [1]), as this computational strategy does not incorporate, among others, ion-pairing effects.

Table 1. Experimental oxidation potentials (E_{ox}, V vs. Fc/Fc⁺) of **1/2**, **1 sh**, and **1 m/2 m**; experimental and computed differences (Δ) between E_{ox1} and E_{ox2} of **1**, **2** and **1 sh**.[a]

| Parameter	1	2	1 sh
E_{ox1} (model)	0.91	0.64	0.91
E_{ox1}	0.84	0.67	0.91
E_{ox2}	1.22	0.88	0.94
$Δ_{exp}$	0.38	0.21	0.03
$Δ_{B1LYP-40}$ (Δ*)	0.58 (0.37)	0.46 (0.22)	0.28 (0.02)
$Δ_{M06-2X}$ (Δ*)	0.62 (0.38)	0.45 (0.22)	0.24 (0.02)
$Δ_{CAM-B3LYP}$ (Δ*)	0.55 (0.37)	0.45 (0.23)	0.28 (0.02)
$Δ_{B3LYP}$ (Δ*)	0.74 (0.36)	0.59 (0.23)	0.33 (0.02)

[a] Values in parentheses (Δ*) were scaled to experimental data; see Figure S12 in the Supporting Information.

The calculated molecular structures of spirobifluorene **1⁺·** and **2⁺·** show oxidation-induced structural reorganization in only one of the fluorenyl units, with the bond length changes identical to those found in the cation radicals of model compound **1 m⁺·/2 m⁺·** (see Figure S8–S9 in the Supporting Information). Similarly, the accompanying spin/charge density distributions in **1⁺·** and **2⁺·** are largely confined to a single unit (Figure [3]).[10] Calculated molecular structures of dications[16] of **1** and **2** show bond-length changes and spin/charge distributions in each fluorenyl unit that are identical to the changes computed in **1 m⁺·** and **2 m⁺·** (Figures [3] and S10–S11 in the Supporting Information), indicating that **1²⁺** and **2²⁺** represent two spatially separated, electronically decoupled bis-cation radicals.
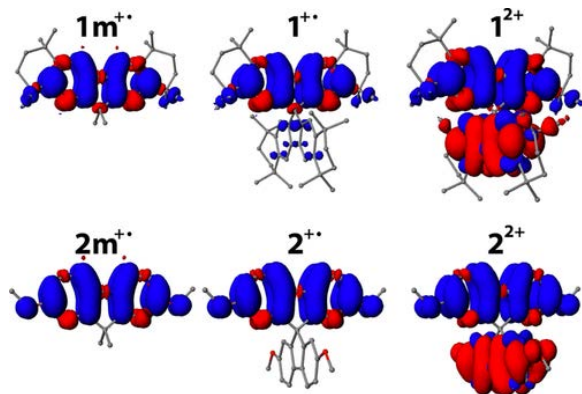
Figure 3 Spin-density isovalue (0.001 au) plots of **1 m$^{+\cdot}$/2 m$^{+\cdot}$**, **1^{+}/2$^{+\cdot}$**, and **1^{2+}/2^{2+}**. The plots show that in **1^{+}/2$^{+\cdot}$**, the charge/spin is mostly distributed over a single fluorene unit and in **1^{2+}/2^{2+}** the charge/spin distributions from two cationic charges separately occupy two fluorene units.

Unlike the Coulombic interactions between a pair of metal cations, Coulombic interactions in spirobifluorene dications are expected to be dependent on the cationic charge distribution onto the different atoms of the fluorenyl chromophores. For example, natural population analysis (NPA)[17] shows that varied substitution in **1^{2+}** and **2^{2+}** produces a different charge distribution pattern on the aromatic carbons, especially the carbon atoms nearest to each fluorene in **1^{2+}** and **2^{2+}** (indicated by blue dots in Figure **4**), and the partial charge on distant oxygens in **2^{2+}**. The varied charge distributions in **1^{2+}** and **2^{2+}** modulate the electrostatic forces (EF) and, in turn, contribute to the observed differences in the splittings Δ in **1^{2+}** and **2^{2+}** (Table **1**).
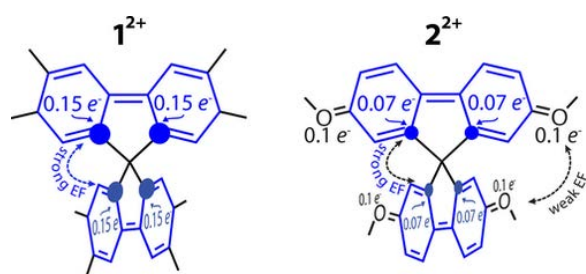
Figure 4 Structures and NPA charges of **1^{2+}** and **2^{2+}**.

As the Coulombic interactions scale inversely with the separation distance between a pair of charged moieties, increasing the interchromophoric separation in spirobifluorene is expected to dramatically reduce the splitting of the oxidation waves (Δ). To systematically probe the distance dependence of the electrostatic interactions, we performed calculations of the relaxed potential energy surface scan on a model bifluorene, where the distance (R) between two fluorenes was varied (Figure **5** A). At each increment, the model bifluorene was optimized at neutral, cation radical, and dication states, which provided the first and second oxidation energies at each separation distance (Figure S15 in the Supporing Information). A plot of the difference between the first and second oxidation energies (Δ) against the interchromophoric distance (R) clearly shows an inverse dependence (Figures **5** B) and a critical distance of 9.3 Å, after which the computed difference Δ (scaled to experimental values) becomes negligible (Figure S16 in the Supporting Information).
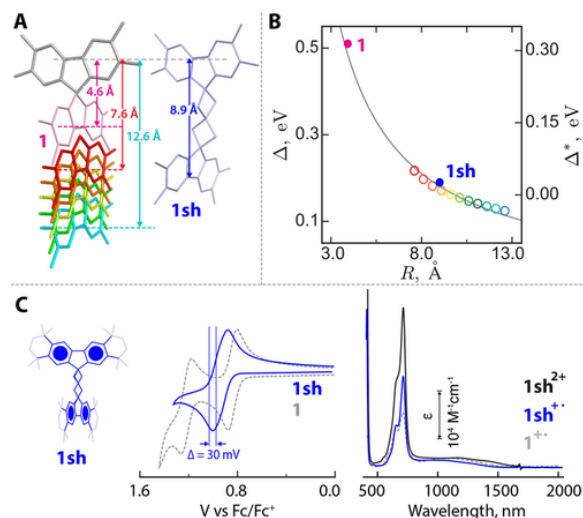
Figure 5 A) Molecular structures of 1, 1 sh, and model bifluorenes (pairs of orthogonally juxtaposed fluorenes) with the interchromophoric distance R (colored arrows) varied in the range of 7.6–12.6 Å between the central C–C bond of each fluorene. B) Plot of the differences between Eox1 and Eox2 against R. Left y-axis denotes computed values (Δ) and right y-axis denotes values scaled to experimental data (Δ^*). C) Cyclic voltammograms of 1 and 1 sh in CH2Cl2 (0.1 m nBu4N+PF6−) at v=200 mV s−1 and 22 °C (left), and electronic absorption spectra of 1+·, 1 sh+·, and 1 sh2+ in CH2Cl2 at 22 °C (right).

Based on the computational scan in Figure **6** B, we sought a spriobifluorene-like molecule, in which two fluorene moities lie further apart, while maintaining the spatial arrangement of the corresponding spirobifluorene. The compound **1 sh,** which incorporates a spiroheptane bridge, represents such a structure with a separation of 8.9 Å between two orthogonal fluorenes (Figure **6**). The separation length is defined as the distance between the biphenyl-like linkages on the fluorene units. The cyclic voltammogram of **1 sh** shows two closely spaced waves (Δ=30 mV), with a splitting one order of magnitude smaller than that of **1**(Δ=380 mV), which attests to the dramatically reduced electrostatic interactions in **1 sh^{2+}**(Figure **6** C). The absorption spectra of **1$^{+·}$** and **1 sh$^{+·}$** are similar, and the absorption spectrum of dication **1 sh^{2+}** is also similar to that of radical cation **1 sh$^{+·}$**, except molar absorptivity for the dication was roughly twice that of **1 sh$^{+·}$**. This suggests an absence of discernable electronic coupling among the cationic fluorenes in **1 sh^{2+}** (Figure **6** C).

The experimental/computational demonstration of severely diminished electrostatic interactions between the cationic fluorenes separated by 8.9 Å in **1 sh^{2+}** agrees well with the observation of a complete absence of the electrostatic interactions amongst circularly arrayed electro-active groups in hexaarylbenzene derivatives (**B** and **C** in Figure **6**), which bear separations of about 8.8 Å. While an approximate distance of 9 Å seems reasonable based on experimental data (Figure **6** and Figure **6**), the characteristic interchromophoric distance where electrostatic interactions are absent is expected to depend on the size, electronic structure of the chromophore, the solvation, and ion pairing.[11, 18]

It is well known that electrostatic interactions among charged species are modulated by solvation; polar solvents shield the charge and reduce the effective Coulombic interactions among the charged species.[18] A compilation of the square wave (SW) voltammograms of spirobifluorene **1** in pure CH$_2$Cl$_2$ and mixtures of CH$_2$Cl$_2$/CH$_3$CN (Figure **6** A) shows that solvent mixtures containing polar CH$_3$CN

reduce the splitting of the oxidation waves in **1** from 380 mV (CH_2Cl_2/CH_3CN=1:0) to 330 mV (CH_2Cl_2/CH_3CN=0.75:0.20), 300 mV (CH_2Cl_2/CH_3CN=0.5:0.5), and 260 mV (CH_2Cl_2/CH_3CN=0.25:0.75).
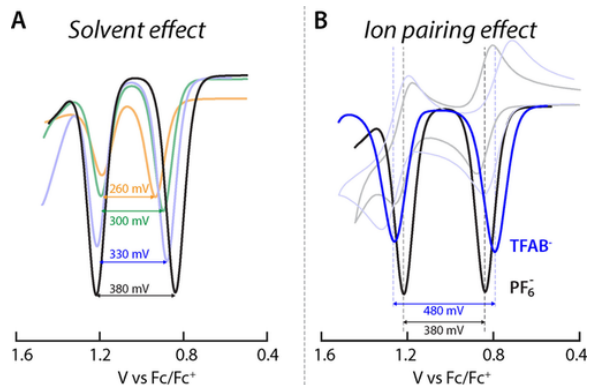
Figure 6 A) Square-wave voltammograms of **1** in CH_2Cl_2/CH_3CN mixtures. 1.0:0.0 (black), 0.75:0.20 (blue), 0.5:0.5 (green) and 0.25:0.75 (yellow) (0.1 m $nBu_4N^+PF_6^-$) at 22 °C. Note that **1** was not very soluble in pure CH_3CN. B) Square-wave of **1** in CH_2Cl_2 obtained in the presence of 0.1 m $nBu_4N^+PF_6^-$ (black curves) or 0.1 m nBu_4N^+TBAF (blue curves) as electrolyte at v=200 mV s^{-1} and 22 °C. Corresponding cyclic voltammograms are shown in gray.

Finally, the role of ion pairing can be examined by employing electrolytes with non-coordinating anions, such as *tetrakis*(pentafluorophenyl)borate (TFAB$^-$), which are known to significantly reduce the effects of ion pairing in comparison to traditionally utilized PF_6^- salts.[11, 18] A decrease in ion pairing should lead to a more naked charge, and therefore result in enhanced electrostatic interactions and increased separation between the oxidation waves. A comparison of the square wave/cyclic voltammograms of **1** in CH_2Cl_2 containing 0.1 m $nBu_4N^+PF_6^-$ (black curves in Figure **7** B) and 0.1 m $nBu_4N^+TFAB^-$ (blue curves in Figure **7** B) showed that the splitting between oxidation waves increases from 380 to 480 mV. This demonstration of the increased splitting of the oxidation waves (Δ) in the presence of a non-coordinating counteranion suggests that an additional decrease in the ion pairing could lead to an experimentally observed value of Δ that approaches those obtained by DFT calculations, which do not account for ion pairing (Table **1**).

In summary, in this study, we used spirobifluorene and its derivatives as a bichromophoric, electronically decoupled model system, which demonstrates that the Coulombic (electrostatic) forces are largely[14] responsible for increasing the second oxidation potential as high as 0.4 V when compared to its first oxidation potential under ambient conditions. An experimental/DFT analysis of the electronic structures of the radical cations and dications of the spirobifluorene showed that atomic charges in fluorenyl chromophores dramatically vary depending on the alkyl and methoxy substitution, which in turn lead to the modulation of electrostatic interactions in the range of 0.2–0.4 V, depending on the substituent. Furthermore, application of the potential energy surface scan and electrochemical/optical spectroscopic analysis of a spirobifluorene derivative, in which two orthogonal fluorenes lie at a distance of 8.9 Å, demonstrated that the Coulombic interactions reach negligible values greater than about 9 Å.

This quantitative finding of the impact of electrostatic forces in modulation of the higher oxidation potentials should aid in the design of novel molecular assemblies for long-range charge-transfer by judicious placement of the charges in the proximity of donors and acceptors in a vein similar to that employed by nature.[19, 20] The design and study of such molecular assemblies is being actively pursued.

Conflict of interest

The authors declare no conflict of interest.

References

1 Facchetti, A., *Chem. Mater.* 2011, **23**, 733.

2 Davis, W. B., Svec, W. A., Ratner, M. A., Wasielewski, M. R., *Nature* 1998, **396**, 60.

3 Shukla, R., Lindeman, S. V., Rathore, R., *Org. Lett.* 2007, **9**, 1291.

4 Navale, T. S., Thakur, K., Vyas, V. S., Wadumethrige, S. H., Shukla, R., Lindeman, S. V., Rathore, R., *Langmuir* 2012, **28**, 71.

5 Rathore, R., Burns, C. L., Deselnicu, M. I., *Org. Lett.* 2001, **3**, 2887.

6 Chebny, V. J., Dhar, D., Lindeman, S. V., Rathore, R., *Org. Lett.* 2006, **8**, 5041.

7 Through-bond electronic coupling between the electroactive groups in **B** and **C** is absent owing to the tri-phenylene spacer, where the central phenylene lies perpendicular to adjacent phenylene. See Sun, D., Lindeman, S. V., Rathore, R., Kochi, J. K., *J. Chem. Soc. Perkin Trans. 2* 2001,1585– 1594.

8 Saragi, T. P., Spehr, T., Siebert, A., Fuhrmann-Lieker, T., Salbeck, J., *Chem. Rev.* 2007, **107**, 1011.

9 Yip, W. T., Levy, D. H., Kobetic, R., Piotrowiak, P., *J. Phys. Chem. A* 1999, **103**, 10.

10 A lowering of E_{ox1} (by 70 mV) of **1** as compared to **1 m** (Figure 2 A), and a minor spillover of the charge/spin density onto the second fluorene unit in **1$^{+\cdot}$** (Figure 3), implies the unexpected occurrence of minor electronic coupling between the orthogonal fluorenyl rings. This unusual observation will be investigated in a future study.

11 Talipov, M. R., Boddeda, A., Hossain, M. M., Rathore, R., *J. Phys. Org. Chem.* 2016, **29**, 227.

12 Talipov, M. R., Hossain, M. M., Boddeda, A., Thakur, K., Rathore, R., *Org. Biomol. Chem.* 2016,**14**, 2961.

13 Rathore, R., Burns, C. L., Deselnicu, M. I., *Org. Synth.* 2005, **82**, 1.

14 The presence of a minor electronic coupling in **1** may be responsible for its decreased oxidation potential by 70 mV as compared to **1 m**, and thus the splitting of the oxidation waves in **1** by 380 mV could represent a contribution from both electronic coupling (70 mV) and Coulombic repulsion (310 mV).

15 Ivanov, M. V., Chebny, V. J., Talipov, M. R., Rathore, R., *J. Am. Chem. Soc.* 2017, **139**, 4334.

16 Singlet states of **1^{2+}** and **2^{2+}** are found to be spin-contaminated (i.e. <S^2>=0.5–0.6 after annihilation). Triplet states of **1^{2+}** and **2^{2+}** are found to be higher in energy by 0.34 and 0.05 kcal mol^{-1}, respectively, than singlet states; see Table S2 in the Supporting Information.

17 Reed, A. E., Weinstock, R. B., Weinhold, F., *J. Chem. Phys.* 1985, **83**, 735.

18 Geiger, W. E., Barrière, F., *Acc. Chem. Res.* 2010, **43**, 1030.

19 Gray, H. B., Winkler, J. R., *Proc. Natl. Acad. Sci. USA* 2015, **112**, 10920.

20 Moore, G. R., Pettigrew, G. W., Rogers, N. K., *Proc. Natl. Acad. Sci. USA* 1986, **83**, 4998.